Molecular Therapy
Oncology
Original Article

circ-1584 selectively promotes the antitumor activity of the oncolytic virus M1 on pancreatic cancer

Taofang Hao,[1,6] Yuanyuan Li,[1,6] Qianyao Ren,[1] Ying Zeng,[1] Leyi Gao,[1] Wenbo Zhu,[1] Jiankai Liang,[1] Yuan Lin,[1,2,3] Jun Hu,[1] Guangmei Yan,[1] Shuxin Sun,[4] and Jing Cai[1,5]

[1]Department of Pharmacology, Zhongshan School of Medicine, Sun Yat-sen University, Guangzhou, China; [2]Advanced Medical Technology Center, The First Affiliated Hospital-Zhongshan School of Medicine, Sun Yat-sen University, Guangzhou, China; [3]Key Laboratory of Human Microbiome and Elderly Chronic Diseases, Ministry of Education, Beijing, China; [4]Pancreatic Center, Guangdong Provincial People's Hospital, Guangzhou, China; [5]Department of Molecular Biology and Biochemistry, Zhongshan School of Medicine, Sun Yat-sen University, Guangzhou, China

Pancreatic cancer is among the most challenging tumors to treat, and due to its immune tolerance characteristics, existing immunotherapy methods are not effective in alleviating the disease. Oncolytic virus therapy, a potential new strategy for treating pancreatic cancer, also faces the limitation of being ineffective when used alone. Elucidating the key host endogenous circular RNAs (circRNAs) involved in M1 virus-mediated killing of pancreatic ductal adenocarcinoma (PDAC) cells may help overcome this limitation. Here, we report that the oncolytic virus M1, a nonpathogenic alphavirus, exhibits different cell viability-inhibitory effects on different pancreatic cancer cells in the clinical stage. Through high-throughput circRNA sequencing, we found that circRNA expression varies among these cells. Further gain-of-function and loss-of-function experiments have shown that circ-1584 can selectively enhance the anti-pancreatic cancer effects of the M1 virus *in vitro* and *in vivo*. Additionally, circ-1584 may negatively regulate miR-578 to modulate the anti-pancreatic cancer effects of the M1 virus. Our findings lay the foundation for using circRNA as an adjuvant to enhance the M1 virus efficacy against pancreatic cancer.

INTRODUCTION

Pancreatic cancer ranks among the top 10 cancers in terms of both incidence and mortality, with a mortality incidence ratio approaching 1.[1,2] The 5-year survival rate in the United States is approximately 13%, while in China it is only 7.2%.[1,3] Pancreatic ductal adenocarcinoma (PDAC) accounts for over 90% of exocrine pancreatic cancers, making it the most common form of pancreatic cancer.[4] Following surgical treatment, the remission rate for PDAC patients using current radiotherapy and chemotherapy drugs is less than 10%, and these patients are prone to drug resistance.[5] Being the most immuno-resistant type of tumor, PDAC does not benefit from immunotherapy, except for less than 1% of patients with microsatellite instability-high tumors who respond to US Food and Drug Administration (FDA)-approved immunotherapy.[6] Due to the recalcitrant nature of PDAC, it is essential to identify new therapeutic targets and develop specific drugs for pancreatic cancer.

As an emerging immunotherapy modality, oncolytic viruses (OVs) can specifically replicate within tumor cells, lyse them, and induce tumor-specific inflammatory responses, potentially overcoming PDAC immune tolerance.[7,8] Currently, the OV T-VEC (talimogene laherparepvec)[9] for melanoma and Delytact[10] for malignant glioma have been clinically approved, but no significant control effect on PDAC has been reported.[11,12] The OV M1, a nonpathogenic alphavirus, has obtained orphan drug designation from the FDA. It is currently undergoing a series of anti-tumor clinical trials in patients with solid tumors (ClinicalTrials.gov: NCT06046742, NCT04665362, and NCT06368921). The M1 virus has shown potential for PDAC therapy both alone and in combination with other treatments.[13–15] The M1 virus does not kill all pancreatic cancer cells,[14,15] and the reasons for this inconsistent cytotoxicity are not well understood. The underlying mechanisms require further investigation.

Circular RNAs (circRNAs) are covalently closed endogenous biomolecules in eukaryotes, classified as non-coding RNAs, and play roles in regulating various diseases.[16,17] circRNAs also regulate the progression of PDAC; for example, circRTN4 promotes the elevation of oncogenic lncRNA HOTTIP expression by adsorbing miR-497-5p, promotes epithelial-mesenchymal transition transformation of PDAC cells, and accelerates PDAC progression.[18] Other circRNAs that promote PDAC progression include circSLIT2[19] and

Received 24 June 2024; accepted 13 December 2024;
https://doi.org/10.1016/j.omton.2024.200919.

[6]These authors contributed equally

Correspondence: ShuXin Sun, Pancreatic Center, Guangdong Provincial People's Hospital, Guangzhou 510080, China.
E-mail: sunshuxin@gdph.org.cn
Correspondence: Jing Cai, Department of Molecular Biology and Biochemistry, Zhongshan School of Medicine, Sun Yat-sen University, Guangzhou 510080, China.
E-mail: caij53@mail.sysu.edu.cn

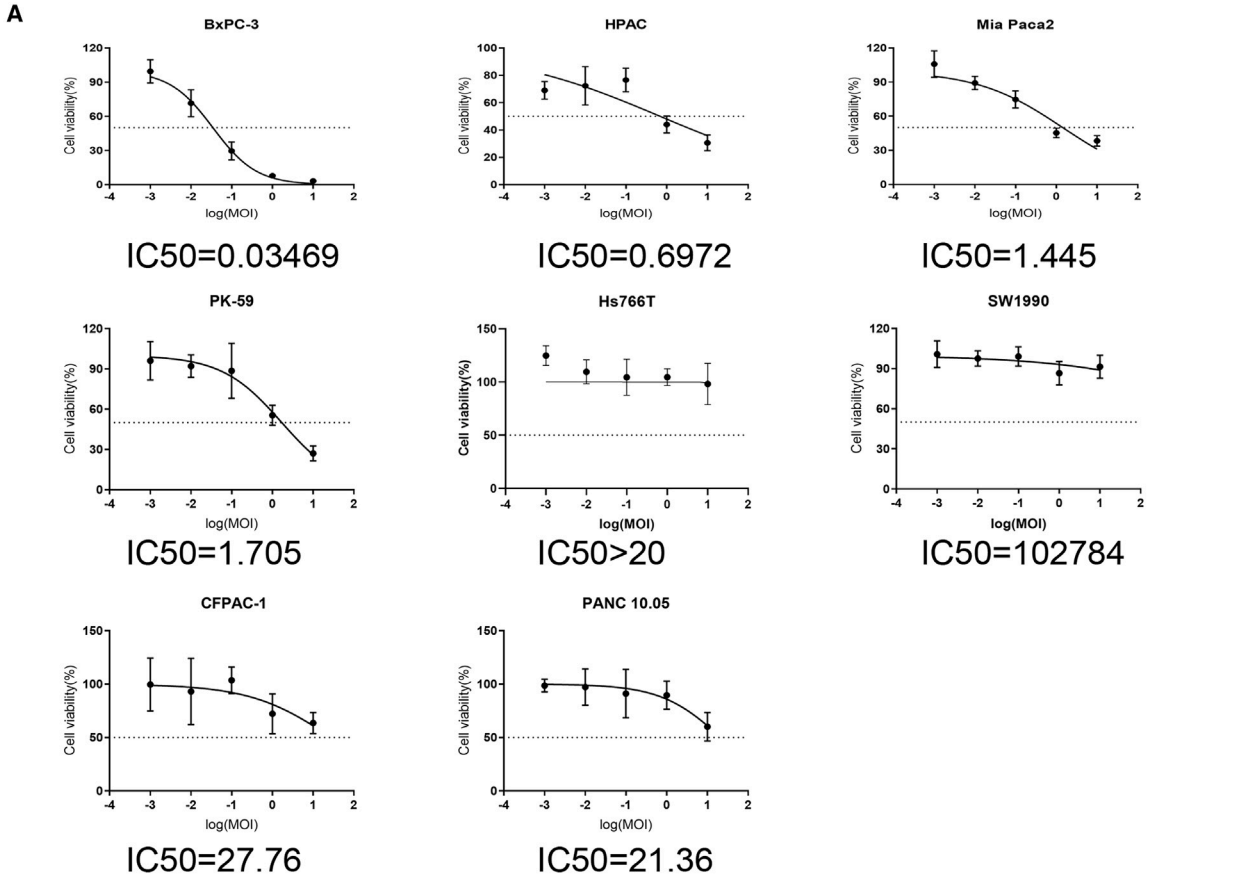

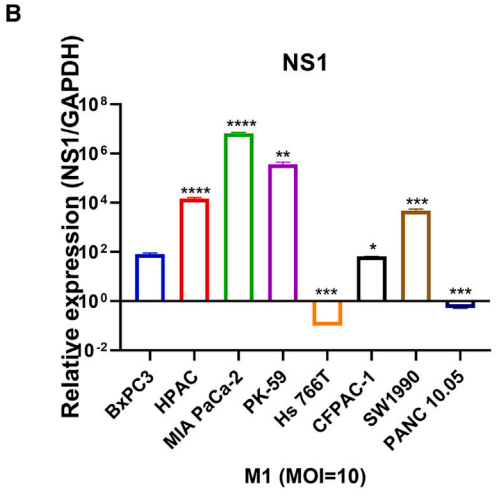

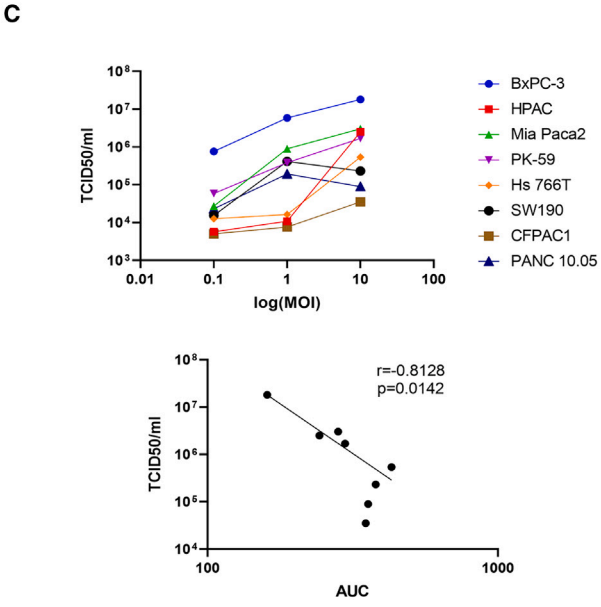

(legend on next page)

circFOXK2,[20] while circNFIB1,[21] hsa_circ_001587,[22] and circ_0047744,[23] among others, can inhibit the progression of PDAC.[24] circRNAs are involved in innate immune responses.[25] circRNAs can induce antiviral immune responses to inhibit viral infections; conversely, viral infections can lead to the generalized degradation of circRNAs.[26] The circRNA AIVR promotes the expression of CREB binding protein by adsorbing miR-330-3p, inducing the production of interferon β, and ultimately inhibiting vesicular stomatitis virus (VSV) infection.[27] On the contrary, after VSV infects host cells, viral RNA competitively binds to NF90/NF110, resulting in reduced expression of circPOLR2A and circDHX34.[28] Overexpression of circRNAs may also promote the replication of viruses in host cells; for instance, circ_0050463 overexpression promotes the replication of influenza A virus in A549 cells,[29] and circPSD3 enhances the replication of Hepatitis C Virus and dengue virus in infected host cells.[30] Due to the complex interactions between viruses and circRNAs, host endogenous circRNAs may be key elements for the OV M1 to function in PDAC cells.

In this study, we observed that the M1 virus exhibited different cell viability inhibition effects on different human pancreatic cancer cells, with circRNA expression varied between BxPC-3 and Hs 766T cells. circRNA sequencing (circRNA-seq) revealed a general reduction in intracellular circRNAs following M1 virus infection. A large number of differentially expressed circRNAs were identified in M1 virus-infected Hs 766T cells and BxPC-3 cells, among which circ-1584 became a key circRNA for the M1 virus to inhibit PDAC cell viability. Overexpression of circ-1584 enhances the inhibition of the viability of the M1 virus against CFPAC-1 and Hs 766T cells and promotes replication of the M1 virus in these cells. Moreover, intratumoral injection of a circ-1584-overexpressing lentivirus has been shown to enhance the anti-tumor effect of the M1 virus *in vivo*, indicating that circ-1584 can be used as an adjuvant to boost the antitumor efficacy of the M1 virus. circ-1584 can directly bind to miR-578, inhibit the expression of miR-578, and thereby affect the expression of downstream genes such as CLCN6, ZNF117, HABP4, and RARB to positively regulate the function of the M1 virus in pancreatic cancer. This study provides a detailed understanding of the roles of circRNAs in treating PDAC with the OV M1 virus and offers novel insights to enhance the oncolytic effect of the M1 virus in PDAC by overexpressing circ-1584.

RESULTS

The M1 virus has different inhibitory effects on the viability of different pancreatic cancer cells

We tested the viability of eight human pancreatic cancer cell lines (BxPC-3, MIA PaCa2, HPAC, PK-59, Hs 766T, SW1990, CFPAC-1, PANC 10.05) after 48 h of treatment with various titers of M1 virus. As shown in Figure 1, the M1 virus exhibits different levels of cell viability inhibition against different pancreatic cancer cell lines. The half maximal inhibitory concentration (IC_{50}) values were less than 10 MOI (multiplicity of infection) in BxPC-3, MIA PaCa2, HPAC, and PK-59 cells, while those with IC_{50} values greater than 20 were Hs 766T, SW1990, CFPAC-1, and PANC 10.05 cells (Figure 1A). Based on these results, we classified BXPC-3, MIA PaCa2, HPAC, and PK-59 as M1-sensitive pancreatic cancer cells, while Hs 766T, SW1990, CFPAC-1, and PANC 10.05 were classified as M1-insensitive pancreatic cancer cells. We further analyzed the amount of M1 viral genome by detecting the expression of the nonstructural gene NS1. The results showed that, after being infected with the same titer of M1 virus, the viral genomes present differently in different pancreatic cancer cells (Figure 1B). Moreover, we detected the viral titer in the culture medium, which provides a more accurate reflection of M1 virus infection and replication than measuring the expression of the M1 virus gene NS1 in cells. We collected the cell culture supernatant 72 h post infection with the M1 virus and detected the viral titer in BHK-21 cells. Following M1 virus infection, the viral titer in the supernatant of M1-sensitive BxPC-3, MIA PaCa2, and PK-59 cells was elevated (Figure 1C). At the same time, we performed a correlation analysis between the viral titer and the area under the cell viability curve (AUC), revealing that higher viral titers were associated with smaller AUC values, indicating that cell viability inhibition was due to viral replication (Figure 1C).

A large number of differentially expressed circRNAs in BxPC-3 and Hs 766T cells after M1 virus treatment

To evaluate whether circRNAs play an important role in the effect of M1 virus on inhibiting PDAC cell viability, we treated BxPC-3 cells (an M1-sensitive pancreatic cancer cell line) and Hs 766T cells (an M1-insensitive pancreatic cancer cell line) with 1 MOI M1 virus, followed by circRNA high-throughput sequencing (Figures 2A and 2B). Compared to BxPC-3 cells, Hs 766T cells exhibited a large number of differentially expressed circRNAs, with 557 downregulated and 410 upregulated. Compared to M1 virus-infected BxPC-3 cells, 319 circRNAs were downregulated and 194 circRNAs were upregulated in M1 virus-infected Hs 766T cells. Comparing M1 virus-infected and uninfected BxPC-3 cells, 179 circRNAs were downregulated, and 105 circRNAs were upregulated. In Hs 766T cells, 176 circRNAs were downregulated, and 72 circRNAs were upregulated (Figure 2C). The differential circRNAs are distributed across all chromosomes but are most abundant on chromosomes 1 and 2 (Figure 2A). The length of circRNA transcripts is mainly concentrated around 500 bp (Figure 2B).

We first selected circRNAs that were differentially expressed between BxPC-3 and Hs 766T cells as well as between M1 virus-infected

Figure 1. Pancreatic cancer cells respond differently to M1 virus treatment

(A) After M1 virus infection of pancreatic cancer cells at different titers for 48 h, the viability was detected by MTT assay. (B) After 48 h of M1 virus infection, expression of the M1 virus gene NS1 in pancreatic cancer cells was detected by qPCR. Each type of cell not infected with the M1 virus was used as a CTL, with the expression of NS1 normalized to 1; values less than 0.0001 were normalized as 0.1. (C) Top: viral titers in the supernatant of pancreatic cancer cell culture medium after M1 virus infection were detected. Bottom: correlation analysis of viral titer and AUC. Data are presented as means ± SD (*$p < 0.05$, **$p < 0.01$, ***$p < 0.001$, ****$p < 0.0001$).

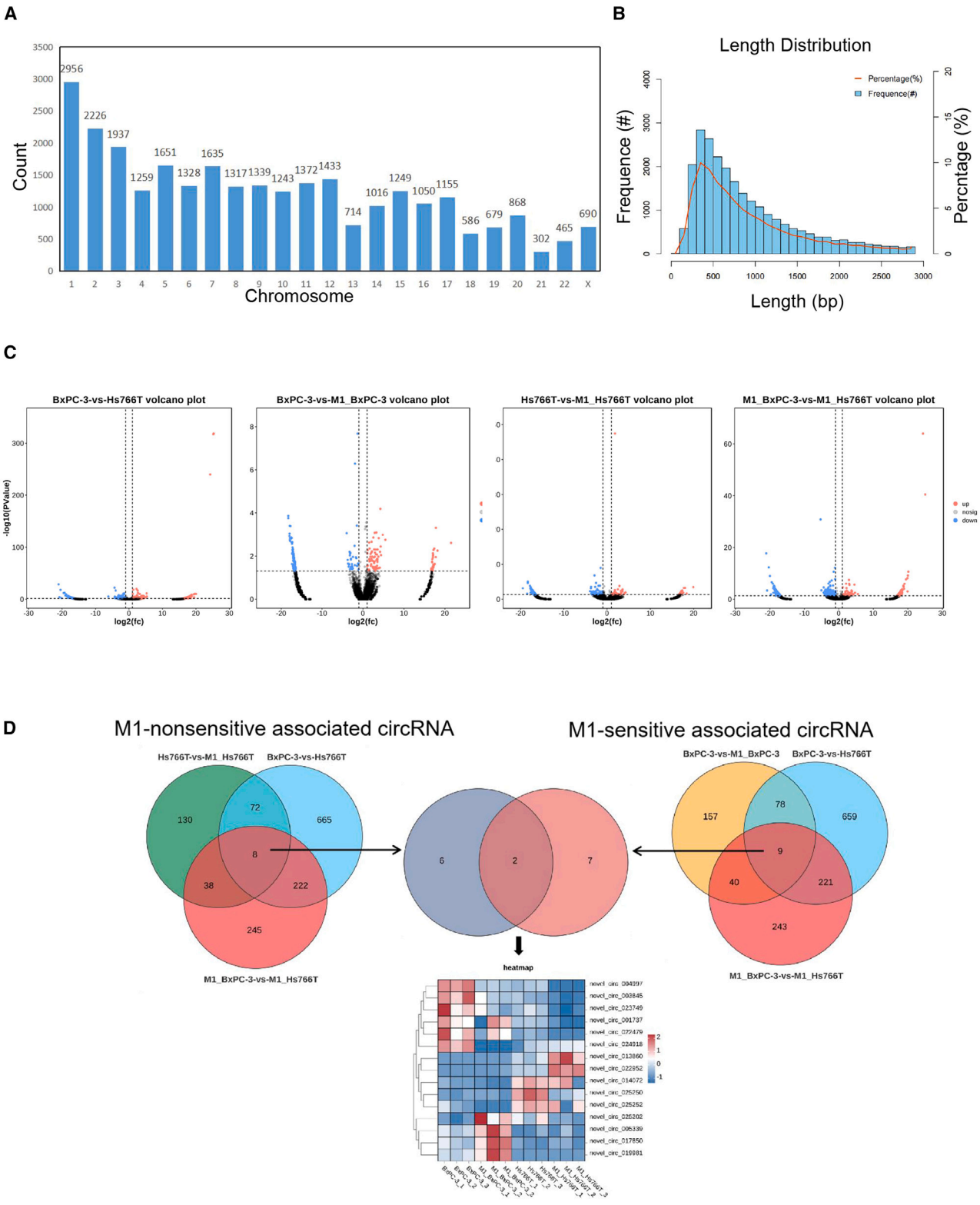

(legend on next page)

BxPC-3 and M1 virus-infected Hs 766T cells, resulting in a total of 230 circRNAs. We then intersected these 230 circRNAs with those differentially expressed in BxPC-3 vs. M1_BxPC-3 (sensitive) and Hs 766T vs. M1_Hs 766T (insensitive), resulting in 15 circRNAs (Figure 2D; Table S1). We then verified the expression of these 15 circRNAs in BxPC-3, M1 virus-infected BxPC-3, Hs 766T, and M1 virus-infected Hs 766T cell samples (Figures 3A and S1). Only the expression of circ-1584 (hsa_circ_0031584) was consistent with the sequencing results, showing higher expression in BxPC-3 cells and a significant decrease after M1 virus treatment. Additionally, circ-1584 expression was higher in M1 virus-infected BxPC-3 cells compared to M1 virus-infected Hs 766T cells (Figure 3A).

Moreover, the back-splicing junction of circ-1584 was verified by Sanger sequencing (Figure 3B). Using 1% agarose gel electrophoresis, we detected the PCR products of BxPC-3 genomic DNA and cDNA and found that only cDNA could detect circ-1584 using divergent primers (Figure 3B). After treating RNA with RNase R, the expression of circ-1584 did not reduce, unlike the relative linear RNA *ARHGAP5* (Figure 3B). This evidence indicates that circ-1584 is a stable circRNA. Then, we examined circ-1584 expression in eight pancreatic cancer cell lines and found that, excluding Mia PaCa2, circ-1584 expression was higher in the sensitive cells (BxPC-3, HPAC, and PK-59) compared to the four less sensitive cell lines (Figure 3C). The expression levels of circ-1584 were reduced in these pancreatic cancer cells infected with the M1 virus, except for except for MIA PaCa2.

These results suggest that circ-1584 may be involved in the regulation of M1 virus inhibition of pancreatic cancer cell viability.

circ-1584 potentiates the viability inhibitory effect of the M1 virus on pancreatic cancer cells

To validate the role of circ-1584 in M1 virus inhibition of PDAC cell viability, we utilized small interfering RNA (siRNA) knockdown of circ-1584 expression and overexpression of circ-1584 using an overexpression plasmid. In the BxPC-3 and PK59 cell lines, which were sensitive to the M1 virus, knockdown of circ-1584 significantly reduced the cell viability mediated by the M1 virus as well as expression of the M1 virus nonstructural gene NS1 and the M1 virus structural protein E1 (Figures 4A and 4C). We also overexpressed circ-1584 in BxPC-3 cells and found that overexpression of circ-1584 increased M1 viral replication and M1-mediated cell viability inhibition (Figure S2A). On the other hand, in the Hs 766T and CFPAC-1 cell lines, which were resistant to the M1 virus, overexpression of circ-1584 significantly increased inhibition of cell viability by the M1 virus, along with a significant increase in the expression of the NS1 gene and E1 protein (Figures 4B and 4D). After knocking down circ-1584 in Hs 766T and CFPAC-1 cells, there was a significant reduction in the expression of the M1 virus gene NS1 and protein E1 within the cells, but this did not diminish the cell viability-inhibitory effect of the M1 virus on these cells (Figures S2B and S2C). The reason may be that the M1 virus itself does not exert an inhibitory effect on the viability of Hs 766T and CFPAC-1 cells. After BxPC-3, Hs 766T, PK-59, and CFPAC-1 cells were treated with circ-1584 siRNA or plasmids for 24 h and then infected with the M1 virus for 72 h, the supernatant of the cell culture medium was harvested, and the viral titer was detected. The results, consistent with Figures 4A–4D and S2A–S2C, demonstrated that overexpression of circ-1584 significantly increased the viral titer of the M1 virus, while knockdown of circ-1584 significantly reduced the viral titer (Figures 4E and S2D).

To determine whether the enhanced M1 viral replication in pancreatic cancer cells affects the oncoselectivity of the M1 virus in non-malignant pancreatic ductal cell lines, we overexpressed circ-1584 in HPDE6-C7 cells, a normal human pancreatic ductal epithelial cell line in which the M1 virus does not inhibit cell viability (Figure S3A). Neither overexpression nor knockdown of circ-1584 in HPDE6-C7 cells increased the inhibitory effect of the M1 virus on cell viability (Figures S3B and S3C).

These findings suggest that circ-1584 enhances the M1 virus-mediated inhibition of cell viability in pancreatic cancer cells without impacting normal pancreatic ductal epithelial cells.

circ-1584 does not enhance the viability inhibition of other types of cancer cells by the M1 virus

To verify whether circ-1584 also promotes the viability inhibition of the M1 virus on other types of cancer cells, we tested the expression of circ-1584 in non-pancreatic cancer tumor cells that are not sensitive to other M1 viruses (Figures S4A and 5A). The expression of circ-1584 in lung cancer (NCI-H226), breast cancer (MCF7), liver cancer (SK-HEP-1), and colorectal cancer (LoVo, HT-29) is not higher than that in BxPC-3 cells. Additionally, the expression of circ-1584 in SK-HEP-1, NCI-H226, and MCF7 cells was significantly lower than that in BxPC-3 cells (Figure 5A). We then overexpressed circ-1584 in NCI-H226, MCF7, and HK-HEP-1 cells by plasmid transfection (Figure S4B). Overexpression of circ-1584 in NCI-H226 cells enhances the inhibitory effect of the M1 virus on cell viability (Figures 5B–5D). However, the viability of NCI-H226 cells infected with the M1 virus after overexpression of circ-1584 was not lower than that of cells only overexpressing circ-1584. Moreover, the overexpression of circ-1584 cannot significantly increase the expression of the intracellular M1 virus gene and protein after infection with the M1 virus (Figures 5C and 5D). Overexpression of circ-1584 in MCF7 and SK-HEP-1 cells did not significantly promote inhibition of viability of the M1 virus in these cells, nor did it significantly increase the expression of the M1 virus NS1 gene and E1 protein in host cells

Figure 2. A large number of differentially expressed circRNAs in BxPC-3 and Hs 766T cells after M1 virus treatment

(A) The distribution of differentially expressed circRNAs on chromosomes in BxPC-3, Hs 766T, M1_BxPC-3, and M1_Hs 766T cell groups. (B) The distribution of the mature length of circRNAs obtained by sequencing. (C) Differentially expressed circRNAs in four groups of samples. Red and blue indicate increased or decreased expression levels, respectively. (D) A schematic diagram of the screening strategy for circRNAs that may be involved in the anti-pancreatic cancer activity of the M1 virus.

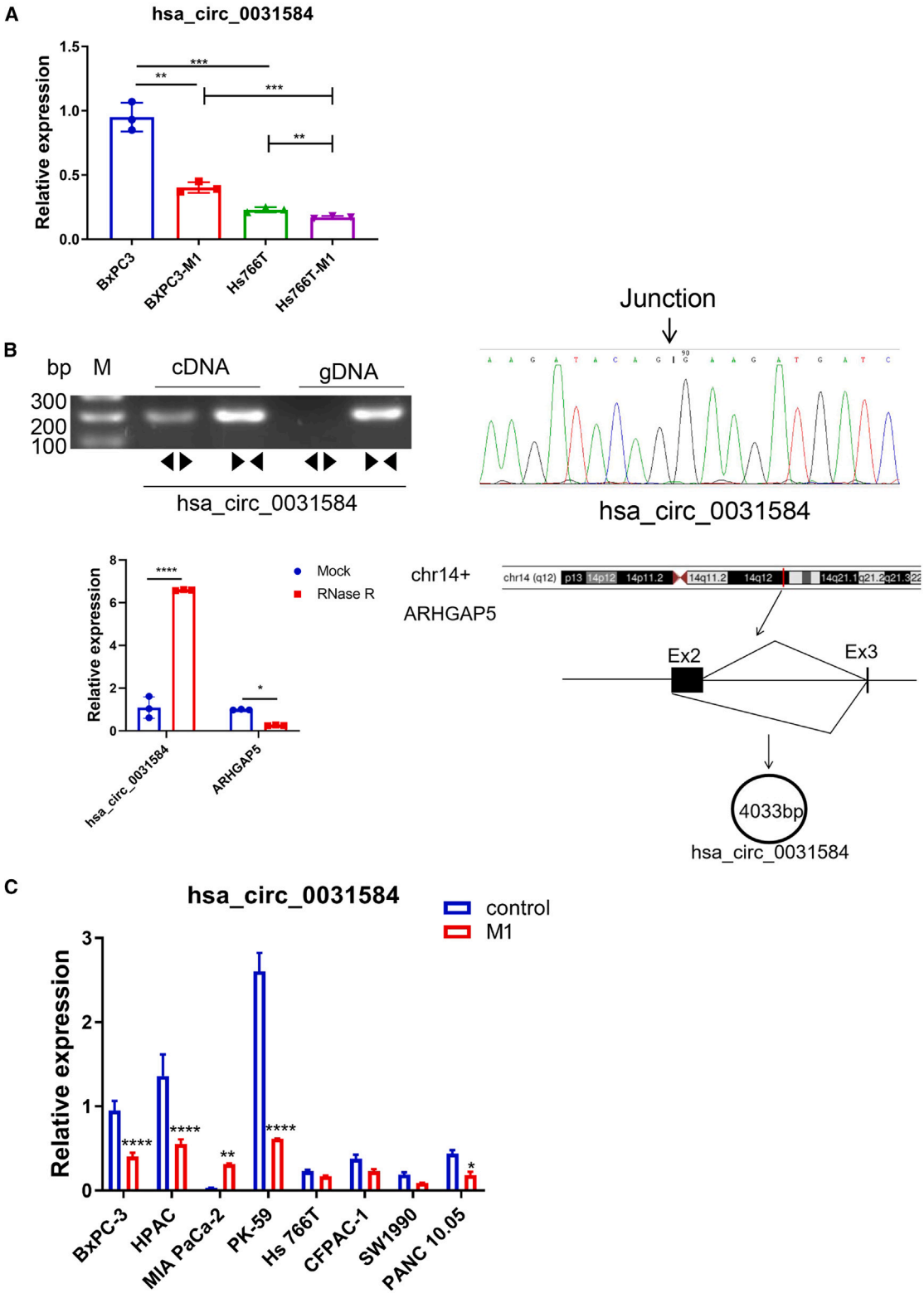

(legend on next page)

(Figures 5C and 5D). These results suggest that circ-1584 may promote the M1 virus's anti-tumor effects only in pancreatic cancer.

circ-1584 promotes the oncolytic effect of the M1 virus in pancreatic cancer *in vivo*

To explore whether overexpression of circ-1584 can promote the anti-tumor effect of the M1 virus in animal models, we established a tumor-bearing model by subcutaneously implanting CFPAC-1 pancreatic cells. When the tumors became palpable, the circ-1584 lentivirus and M1 virus were administered (Figure 6A). Consistent with the results in cellular experiments, the combination of the circ-1584 lentivirus and M1 virus significantly inhibited the tumor growth of CFPAC-1 compared to other groups (Figure 6B). We further detected the expression of circ-1584 and the M1 virus gene NS1 in tumor tissue. As shown in Figure 6C, the circ-1584 lentivirus significantly increased the expression of circ-1584 and significantly increased the expression of the NS1 gene in the tumor. These results suggest that circ-1584 can serve as an adjuvant to enhance the antitumor effect of the M1 virus in treatment of pancreatic cancer.

circ-1584 directly adsorbs and downregulates miR-578 to modulate the anti-pancreatic cancer effects of the M1 virus

circRNAs can regulate the expression of source genes, serve as a natural subcellular localization scaffold, interact with proteins, encode and translate into polypeptides and sponged miRNA, and directly regulate RNA.[31,32] The Circular RNA Interactome website (https://circinteractome.nia.nih.gov/) predicts the ability of circ-1584 to sponge miRNAs. Among these, there are 8 miRNAs with more than 2 binding sites for circ-1584; namely, hsa-miR-1305, hsa-miR-382, hsa-miR-513a-3p, hsa-miR-942, hsa-miR-578, hsa-miR-582-3p, hsa-miR-593, and hsa-miR-607(Table S2).

Next, we detected the expression of hsa-miR-578, hsa-miR-1305, hsa-miR-382, hsa-miR-582-3p, hsa-miR-593, hsa-miR-607, hsa-miR-942, and hsa-miR-513a-3p following circ-1584 overexpression in PK-59 cells. Among the tested miRNAs, only miR-578 showed a significant decrease after circ-1584 overexpression (Figure 7A). These results suggest that circ-1584 may exert its function by downregulating miR-578 expression.

We further utilized biotin-conjugated circ-1584 and miR-578 probes to perform RNA antisense purification (RAP) experiments in BxPC-3 cells. Compared with the DNA control probe (S-probe), the circ-1584-AS probe captured significantly more circ-1584 and miR-578 through RAP. In cells overexpressing circ-1584, the circ-1584-AS probe captured more circ-1584, while the levels of miR-578 captured by circ-1584 were reduced (Figure 7B), consistent with the results shown in Figure 7A, indicating that circ-1584 significantly downregulates miR-578 expression. Similarly, circ-1584 was significantly enriched in complexes with the miR-578 probe compared to the RNA control probe (oligo probe) (Figure 7B). Further, fluorescence *in situ* hybridization (FISH) experiments demonstrated the cytoplasmic co-localization of circ-1584 and miR-578 (Figure 7C). These results suggest that circ-1584 can adsorb miR-578.

To determine whether circ-1584 regulates the anti-pancreatic cancer effects of the M1 virus by downregulating miR-578, CFPAC-1 cells were co-transfected with circ-1584 or vector and miR-578 or mimic-negative control (NC), followed by infection with the M1 virus. Cell viability and viral titers were then measured (Figure 7D). Overexpression of miR-578 in CFPAC-1 cells abrogated the circ-1584-induced enhancement of M1 virus-mediated cell viability inhibition (Figure 7E). Additionally, miR-578 overexpression suppressed the circ-1584-induced increase in M1 viral titers (Figures 7E and 7F).

Furthermore, we utilized miRTarBase (https://miRTarBase.cuhk.edu.cn/) to predict target genes regulated by miR-578 and selected 10 genes (Table S2) that were reported in ≥ 2 literature sources as being regulated by miR-578 for validation. Following miR-578 overexpression in BxPC-3 and CFPAC-1 cells, we assessed the expression of CLCN6, HABP4, RARB, ZNF117, AZI2, HNRNPU, PAPD7, LOH12CR2, STPG1, and HOOK3 using qPCR. We found that only CLCN6, ZNF117, HABP4, and RARB expression was significantly reduced in both cell lines following miR-578 overexpression (Figure S5). Therefore, miR-578 may affect the anti-pancreatic cancer action of the M1 virus by regulating CLCN6, ZNF117, HABP4, and RARB.

In summary, circ-1584 may enhance the anti-pancreatic cancer activity of the M1 virus by adsorbing and downregulating miR-578, which, in turn, upregulates the expression of CLCN6, ZNF117, HABP4, and RARB.

circ-1584 may serve as a precision biomarker for the M1 virus in the treatment of pancreatic cancer

To evaluate the clinical relevance of circ-1584 to PDAC patients, we performed immunohistochemistry (IHC) to detect the expression of Zinc-Finger Antiviral Protein (ZAP), identified as a negative precision marker for predicting the efficacy of the M1 virus[14] in tumor tissues from 20 pancreatic cancer patients. We also used FISH to detect the expression of circ-1584 (Figure 8). We found that the expression of circ-1584 is negatively correlated with that of ZAP, suggesting that patients with low ZAP expression, who are more likely to benefit from

Figure 3. circ-1584 is involved in the regulation of pancreatic cancer cells in response to the M1 virus

(A) qPCR verification of the expression of circ-1584 in four groups of samples. (B) Verification of the cyclization of circ-1584. Top left: the qPCR products amplified by divergent and converged primers of circ-1584 were examined using 1% agarose gel electrophoresis. Top right: the black arrow indicates the back-splicing junction detected by Sanger sequencing. Bottom left: relative expression of circ-1584 and linear ARHGAP5 with or without RNase R treatment in BxPC-3 cells. Bottom right: schematic of circ-1584 formation. (C) qPCR detected the expression of circ-1584 in the eight types of pancreatic cancer cells after M1 virus infection or non-infection. Data are presented as means ± SD (*$p < 0.05$, **$p < 0.01$, ***$p < 0.001$, ****$p < 0.0001$).

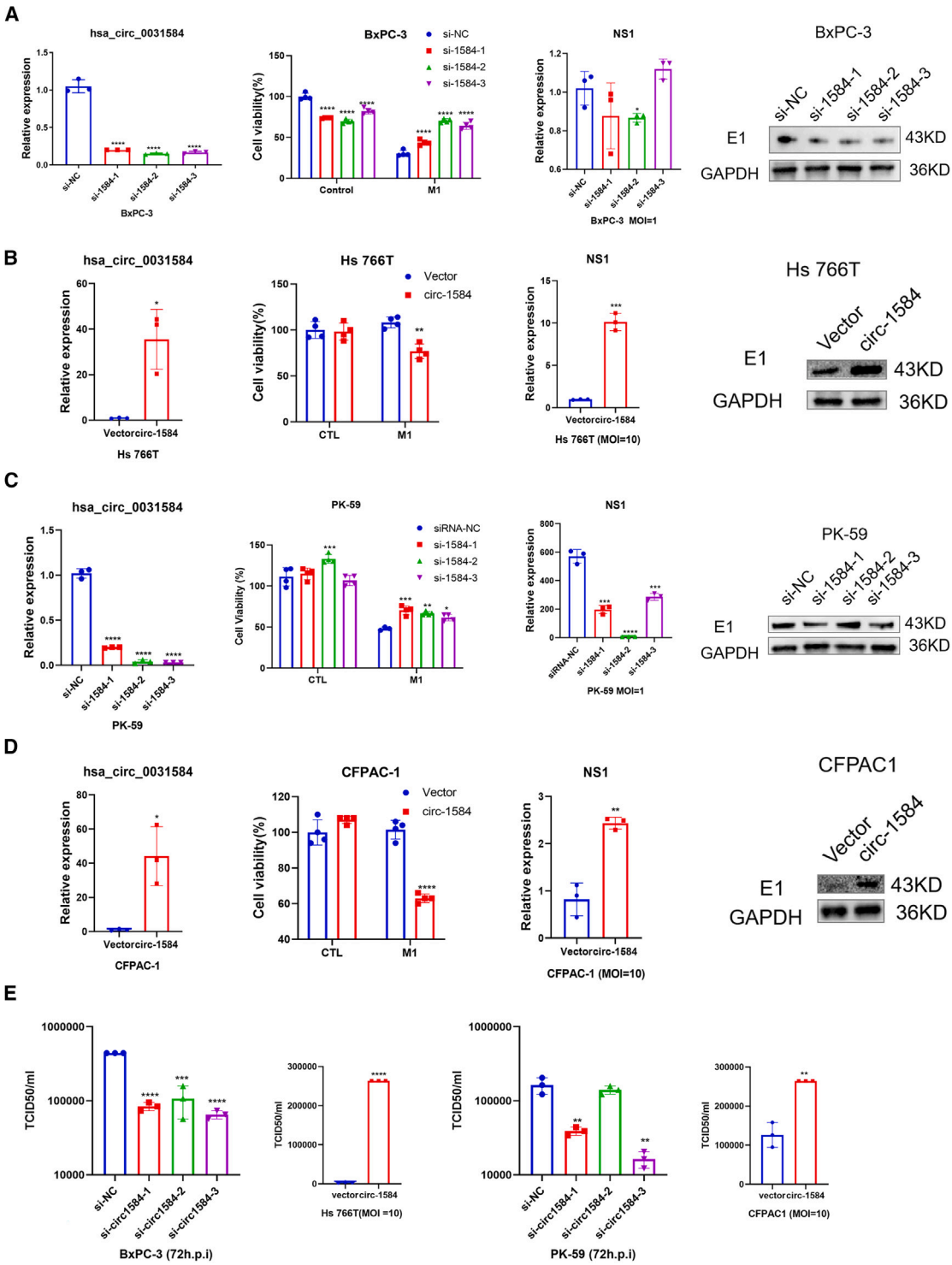

Figure 4. circ-1584 promotes the killing effect of the M1 virus on pancreatic cancer cells

(A and C) BxPC-3 and PK-59 cells were transfected with siRNA-NC or si-circ1584 and then infected with or without the M1 virus. The expression of circ-1584 was detected by qPCR, cell viability was detected by MTT assay, expression of the M1virus gene NS1 was detected by qPCR, and expression of the M1 virus protein E1 was detected by

(legend continued on next page)

M1 virus treatment, may also exhibit high circ-1584 expression. These results indicate that circ-1584 might be used as a biomarker to assess the response to M1 virus treatment.

DISCUSSION

In this study, circ-1584 was identified as a key factor in the differing viability-inhibitory effects of the M1 virus on various pancreatic cancer cells. In BxPC-3 and PK-59 cells, knockdown of circ-1584 inhibited the inhibition of pancreatic cancer cell viability by the M1 virus, while overexpression of circ-1584 in CFPAC-1, Hs 766T, and BxPC-3 cells enhanced the anti-pancreatic cancer effect of the M1 virus. The overexpression of circ-1584 enhances the antitumor effect of the M1 virus, which is specific to pancreatic cancer and does not affect the safety of the M1 virus for normal human pancreatic ductal cells. circ-1584 may exert its anti-pancreatic cancer effect by acting as a sponge for miR-578. Moreover, circ-1584 is negatively correlated with the expression of the antiviral factor ZAP in pancreatic cancer tissue, indicating that circ-1584 also has the potential to serve as a biomarker for predicting the response to M1 virus treatment in pancreatic cancer. Our findings offer new possibilities for enhancing the oncolytic efficacy of the M1 virus against pancreatic cancer.

OVs, as a novel form of immunotherapy, are used to treat tumors primarily by lysing tumor cells and releasing tumor antigens to activate the tumor immune microenvironment.[33] The OV T-VEC, which has been used clinically, may not benefit PDAC patients because it carries granulocyte-macrophage colony-stimulating factor but can promote PDAC cell proliferation.[34] However, T-VEC armed with CD40L can significantly extend the survival rate of PDAC mice.[35] Other OVs that have been approved for marketing, such as Delytact (teserpaturev/G47Δ), are also used in combination with focal adhesion kinase inhibitors and immune checkpoint blockade (ICB) to effectively inhibit PDAC in mice.[36] Our previous studies have shown that combination of the OV M1, NanoKnife (a phosphatidylinositol 3-kinase γ inhibitor), and ICB can more effectively inhibit tumor growth in PDAC mice and prolong their survival rate in mice.[13,37] These results suggest that combined therapy with the M1 virus and other drugs is a promising direction for curing PDAC.

circRNAs can exert their effects in various ways, and we found that circ-1584 may function by inhibiting miR-578. Analysis using the online websites KM plotter (http://kmplot.com/analysis/index.php?p=background) and dbDEMC (https://www.biosino.org/dbDEMC/index) revealed that miR-578 is underexpressed in pancreatic cancer (Table S3), and its low expression is associated with a better prognosis (p = 0.0091). miR-578 can participate in regulating the vitality, apoptosis, colony formation, migration, invasion, angiogenesis, and glycolysis of breast cancer cells.[38,39] miR-578 can regulate the progression of liver cancer by inhibiting the RAB7A and PSME3 genes.[39] miR-578 can also affect the proliferation and migration of osteosarcoma cells by regulating the expression of vascular endothelial growth factor.[40] All of these results suggest that miR-578 can regulate various tumors, including pancreatic cancer. So, how does miR-578 regulate the anti-pancreatic cancer effect of the M1 virus?

The downstream target genes regulated by miR-578 are CLCN6, ZNF117, HABP4, and RARB. CLCN6 (also known as CLC-6) is a member of the voltage-dependent chloride channel protein family, capable of functioning as a chloride channel or a reverse transporter, and its gene mutations can cause severe neurodegenerative diseases.[41,42] Research on CLCN6 in tumors is relatively scarce, with most studies focusing on glioblastoma, and it can also serve as an indicator of prostate cancer recurrence.[43,44] ZNF117 can regulate the Notch signaling pathway by interacting with JAG2, thereby controlling the resistance of glioblastoma to temozolomide treatment.[45] HABP4, hyaluronic acid-binding protein 4, can regulate ribosomal stability, bind with P53, and participate in the transcriptional regulation of numerous genes, thereby controlling the cell cycle and apoptosis.[46,47] Moreover, HABP4 is underexpressed in colorectal cancer.[48] RARB is a member of the retinoic acid receptor family, is underexpressed in pancreatic cancer tissue, and is involved in regulating the mechano-vitality of pancreatic cancer cells.[49] In our sequencing results from BxPC-3 and Hs 766T cells, we also found that RARB is more highly expressed in BxPC-3 cells compared to the M1-insensitive Hs 766T cells. These results suggest that miR-578 may participate in the anti-pancreatic cancer effect of the M1 virus by regulating target genes.

In conclusion, we found that circ-1584 can promote the anti-pancreatic cancer effect of the M1 virus both *in vivo* and *in vitro*. circ-1584 can act as a sponge for miR-578 to promote the expression of downstream genes, thereby enhancing the anti-pancreatic cancer effect of the M1 virus. We also used clinical pancreatic cancer samples to detect the expression of circ-1584 and the biomarker ZAP for response to M1 virus treatment and found that the expression of circ-1584 is negatively correlated with ZAP. The limitation of this article is that we identified CLCN6, ZNF117, HABP4, and RARB as downstream target genes of miR-578, but it has not yet been determined whether these target genes participate in the regulatory role of the circ-1584/miR-578 axis on M1 virus replication and anti-pancreatic cancer effects. Our findings lay a preclinical research foundation for circ-1584 to become an OV adjuvant for treating pancreatic cancer.

MATERIALS AND METHODS

Cell culture and materials

The following human PDAC cell lines were used in this study. BxPC-3 and CFPAC-1 were sourced from the National Collection

western blot (WB). (B and D) Hs 766T and CFPAC-1 cells were transfected with vector or the circ-1584 overexpression plasmid and then infected with or without the M1 virus. The expression of circ-1584 was detected by qPCR, cell viability was detected by MTT assay, expression of the M1 virus gene NS1 was detected by qPCR, and expression of the M1 virus protein E1 was detected by WB. (E) Viral titers in the supernatants of cell culture medium collected after knockdown or overexpression of circ-1584 in BxPC-3, Hs 766T, PK-59, and CFPAC-1 cells were measured. CTL, control. Data are presented as means ± SD (*p < 0.05, **p < 0.01, ***p < 0.001, ****p < 0.0001).

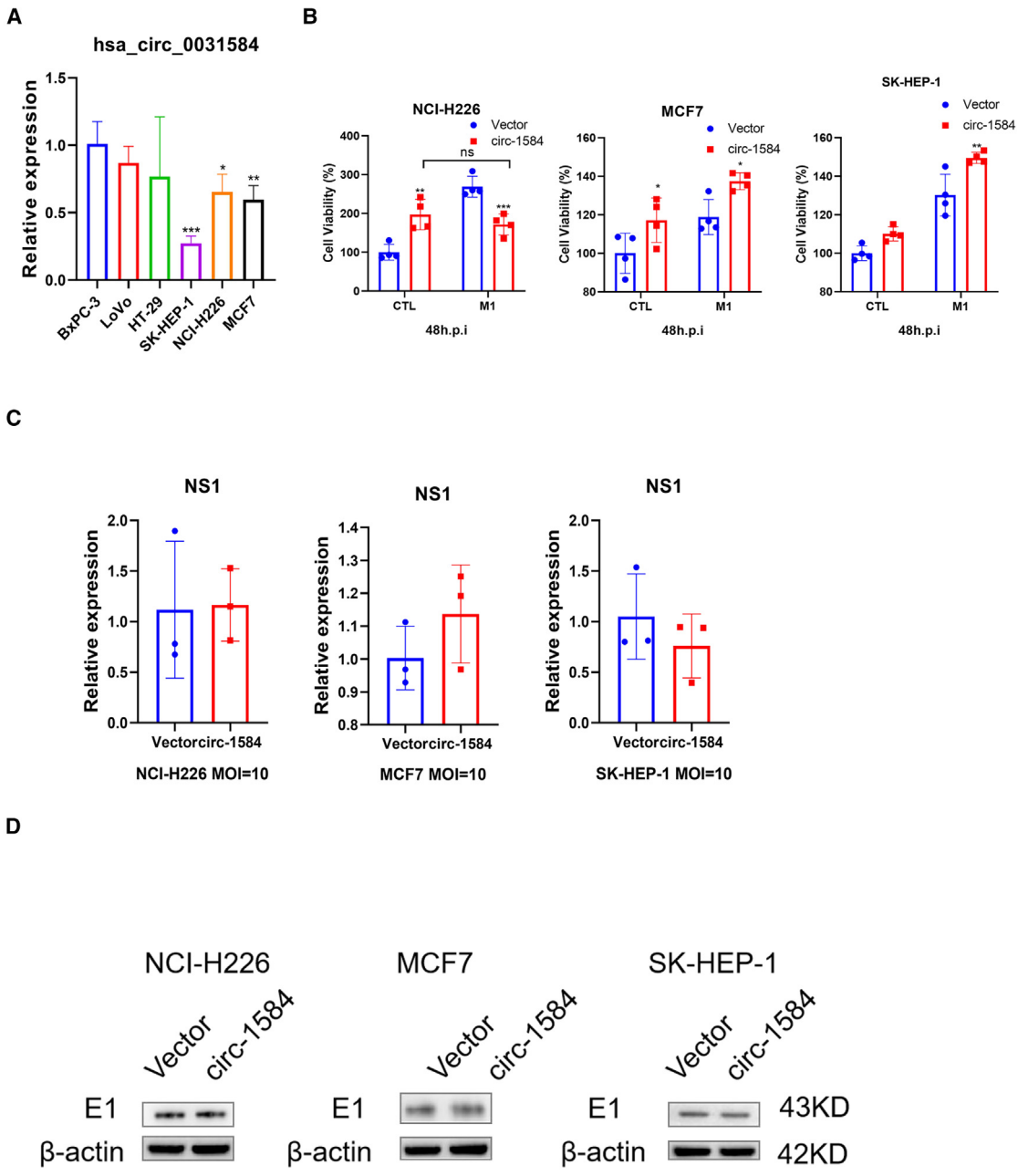

Figure 5. circ-1584 cannot promote M1 virus killing of M1-insensitive non-pancreatic cancer tumor cells

(A) qPCR detected the expression of circ-1584 in M1-insensitive non-pancreatic cancer tumor cells. (B) MTT assay to detect the inhibitory effect of the M1 virus on cell viability after overexpression of circ-1584 in M1-insensitive non-pancreatic cancer tumor cells. (C) After overexpressing circ-1584 in M1-insensitive non-pancreatic cancer cells, qPCR detected the expression of the M1 virus gene NS1. (D) After overexpressing circ-1584 in M1-insensitive non-pancreatic cancer cells, WB detected the expression of the M1 virus protein E1. h.p.i, hours post infection. Data are presented as means ± SD (ns, no significance; $^{*}p < 0.05$, $^{**}p < 0.01$, $^{***}p < 0.001$).

of Authenticated Cell Cultures. Hs 766T, PK-59, and PANC 10.05 were sourced from Cobioer Biosciences. MIA PaCa2, and SW1990 are cell lines maintained in our laboratory. HPAC cells were purchased from Guangzhou Jennio Biotech. HPDE6-C7 cells were purchased from Nanjing Nanoeast Biotech. Lung cancer (NCI-H226), breast cancer (MCF-7), liver cancer (SK-HEP-1), and colorectal cancer (LoVo, HT-29) cells are stored in our laboratory. MCF7, CFPAC-1, SK-HEP-1, HPAC, MIA PaCa-2, Hs766T, HPDE6-C7, and SW1990 cells were maintained in DMEM (Gibco, USA). NCI-H226, BxPC-3, PK-59, and PANC 10.05 were maintained in

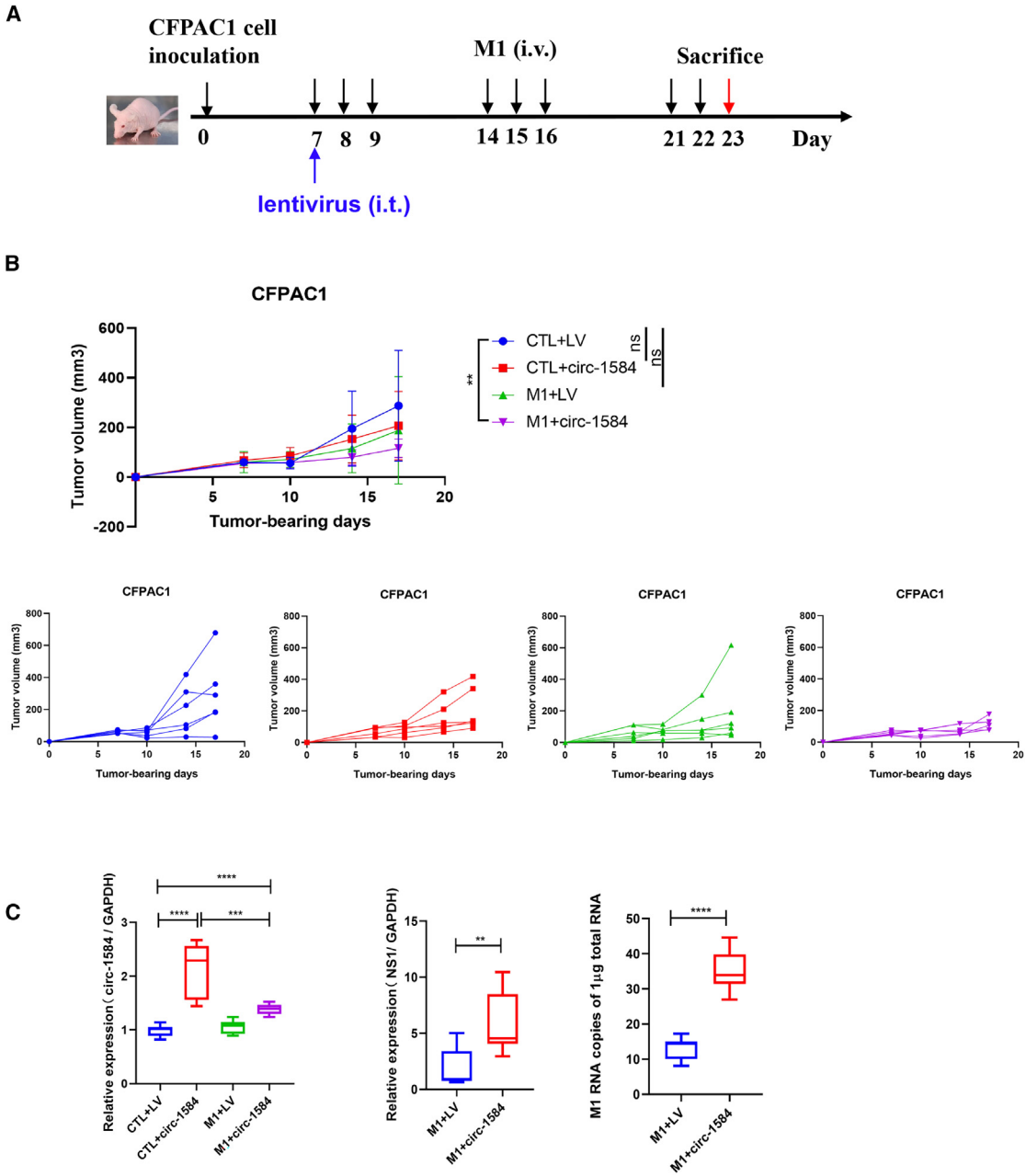

Figure 6. Overexpression of circ-1584 *in vivo* enhances the oncolytic effect of the M1 virus in pancreatic cancer

(A) Schematic of the combination of the M1 virus and lentivirus. Vehicle/M1 virus and lentivirus were administered to nude mice on the 7th day after subcutaneously implanting CFPAC-1 cells. M1 (intravenous, 1×10^7 PFU, 8 times), lentivirus (intratumoral, 1×10^7 PFU, 1 time). (B) Top: average growth curve of mouse tumors in each group. Bottom: growth curves for each mouse in each group ($n = 6$ for each group). (C) Left: qPCR detected the expression of circ-1584 in tumor tissues of mice in each group. Center: qPCR detected the relative expression of the M1 virus gene NS1 in tumor tissues of mice in each group. Right: qPCR detection of M1 virus genome copy number in each group of tumor tissues ($n = 3$ for each group). Data are presented as means ± SD (**$p < 0.01$, ***$p < 0.001$, ****$p < 0.0001$). CTL, vehicle for M1 virus solution; LV, empty lentivirus; circ-1584, circ-1584 overexpression lentivirus.

RPMI 1640 medium (HyClone). LoVo was maintained in Ham's F-12K medium. HT-29 was maintained in McCoy's 5A medium supplemented with 10% fetal bovine serum (Gibco) and 1% penicillin/streptomycin (PS) (Gibco), at 37°C with a 5% CO_2 atmosphere. For all experiments, cells used in this study were passaged no more than 10 times.

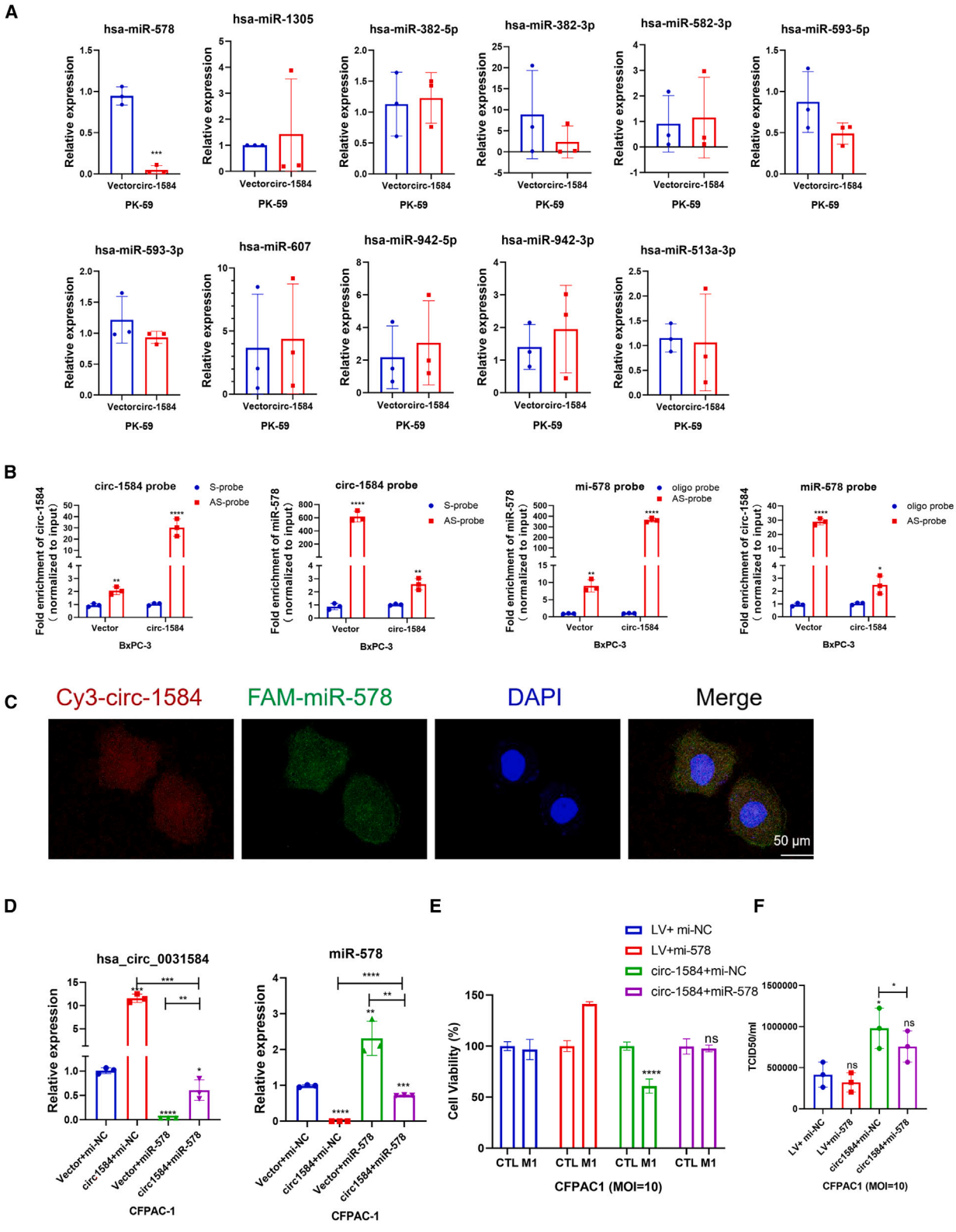

(legend on next page)

Virus production and titer determination

The M1 virus (M1-c6v1 strain) was produced in Vero cells and provided by Guangzhou Virotech Pharmaceutical. The M1 virus was cultured in VP-SFM (Thermo Fisher Scientific) supplemented with 1% (v/v) MEM-NEAA and 2% (v/v) GlutaMAX (Thermo Fisher Scientific). When approximately 80% of the Vero cells were infected and showed a marked cytopathic effect (CPE), the supernatant was collected, centrifuged at 3,000 × *g* and 4°C for 20 min, and stored at −80°C.

The titer of the M1 virus and the titer of the M1 virus in the supernatant of cell culture medium infected with the M1 virus was determined in BHK-21 cells. The virus or the supernatant of the virus-containing culture medium was diluted in nine gradients at a ratio of 10 times and then used to infect BHK-21 cells for 72 h. After infection, the expression of GFP and the presence of CPE were detected using a fluorescence microscope. The virus titer was calculated using the Spearman-Karber method to determine the 50% tissue culture infectious dose ($TCID_{50}$).

Cell viability assay

Cells were seeded in 96-well plates at 3,000 cells per well in 100 μL of medium. After 48–72 h of infection with the M1 virus at different MOIs, 3-(4,5-dimethylthiazol-2-yl)-2,5-diphenyltetrazolium bromide (MTT) was added (5 mg/mL), and the virus was incubated at 37°C for 1–2 h. The MTT-containing medium was removed, and the formazan crystals were dissolved in 100 μL of DMSO. The optical absorbance was measured at 570 nm using a microplate reader (Biotek Synergy H1).

circRNA-seq

Total RNA was extracted using TRIzol reagent (Invitrogen, USA) according to the manufacturer's protocol. RNA quality was assessed on an Agilent 2100 Bioanalyzer (Agilent Technologies, USA) and checked using agarose gel electrophoresis. After total RNA was extracted, rRNAs were removed to retain mRNAs and non-coding RNAs. The enriched mRNAs and non-coding RNAs were fragmented into short fragments and reverse transcribed into cDNA. Second-strand cDNA was synthesized. Next, the cDNA fragments were purified, end repaired, poly(A) added, and ligated to Illumina sequencing adapters. Then, the second-strand cDNA was digested. The digested products were size selected, PCR amplified, and sequenced using Illumina HiSeq 4000 by Gene Denovo Biotechnology (Guangzhou, China). The obtained raw data were filtered to obtain clean data for analysis. Then, rRNA data and mRNA data were removed, and finally circRNA was identified using find_circ and CIRI2 software. EdgeR software was used to compare the expression level of each circRNA between samples.

Quantitative real-time PCR

Total RNA was extracted from tumor cells or tissues using TRIzol reagent following the manufacturer's protocol. RNA was reverse transcribed into cDNA using the Evo M-MLV (Accurate Biotechnology, China). PCR was performed with SuperReal PreMix Plus (SYBR Green) (Tiangen, China), and glyceraldehyde-3-phosphate dehydrogenase (GAPDH) was used as an internal control. qPCR was performed to detect the genomic copy number of M1 virus in tumor tissues using the FastKing one-step RT-qPCR kit (Probe) (Tiangen). The primers and probes are shown in Table S4. The reaction conditions were as follows: initial denaturation 1 cycle, 95°C for 15 s, 60°C for 15 s, 72°C for 30 s, (40 cycles), melting curve 1 cycle, cooling 1 cycle. Data were analyzed according to the comparative $2^{-\Delta\Delta CT}$ method.

RNase R treatment

Total RNA from cells was extracted using TRIzol reagent and subsequently divided into two aliquots. One was used for RNase R digestion, and 2 μg of total RNA was mixed with buffer and incubated for 15 min at 37°C in 2 U/mg RNase R (Beyotime, China). The other aliquot was the control, which was treated with 0.2 μL of diethyl pyrocarbonate water. GAPDH was used as the internal control.

Plasmids, siRNA, cell transfection, lentivirus construction, and stable strain construction

The sequence of human circ-1584 was generated through chemical gene synthesis and cloned into the lentiviral vectors (LV, pCDH-CMV-MCS-EF1-PURO) and pcDNA3.1 plasmid (GENCEFE, Wuxi, China) to construct the overexpression vectors. siRNAs specific to human circ-1584 were synthesized at GENCEFE and used to transiently silence the expression of circ-1584. Mimics of miR-578 and NC mimics were synthesized at GENCEFE. According to the manufacturer's protocol, the aforementioned vectors, siRNA, and mimics were transfected using Lipofectamine 3000 transfection reagent (Invitrogen, USA). The sequences are listed in Table S5. The transfection efficiency of overexpression and knockdown was detected using RT-qPCR.

The LV plasmid and LV-circ1584 plasmid were transfected into HEK293T cells for 72 h, and the medium supernatant was collected. The collected medium supernatant was centrifuged at a speed of

Figure 7. circ-1584 regulates the anti-pancreatic cancer effects of the M1 virus by adsorbing miR-578

(A) After overexpression of circ-1584 in PK-59 cells, qPCR was used to detect the expression of 8 miRNAs. (B) The interaction between circ-1584 and miR-578 was detected by qPCR after RAP of BxPC-3 cell lysates utilizing probes conjugated to biotin with circ-1584 and miR-578. (C) The interaction between circ-1584 and miR-578 was detected by FISH assay using a Cy3 conjugated circ-1584 probe and a FAM-conjugated miR-578 probe in BxPC-3 cells. (D) In CFPAC-1 cells, circ-1584 and miR-578 were overexpressed simultaneously, and the expression of circ-1584 and miR-578 was detected by qPCR. (E) In CFPAC-1 cells, after simultaneous overexpression of circ-1584 and miR-578, the M1 virus was used for infection, and MTT was used to detect CFPAC-1 cell viability. (F) In CFPAC-1 cells, after simultaneous overexpression of circ-1584 and miR-578, the M1 virus was used for infection, and viral titers in the medium supernatant were detected. Data are presented as means ± SD (*$p < 0.05$, **$p < 0.01$, ***$p < 0.001$, ****$p < 0.0001$).

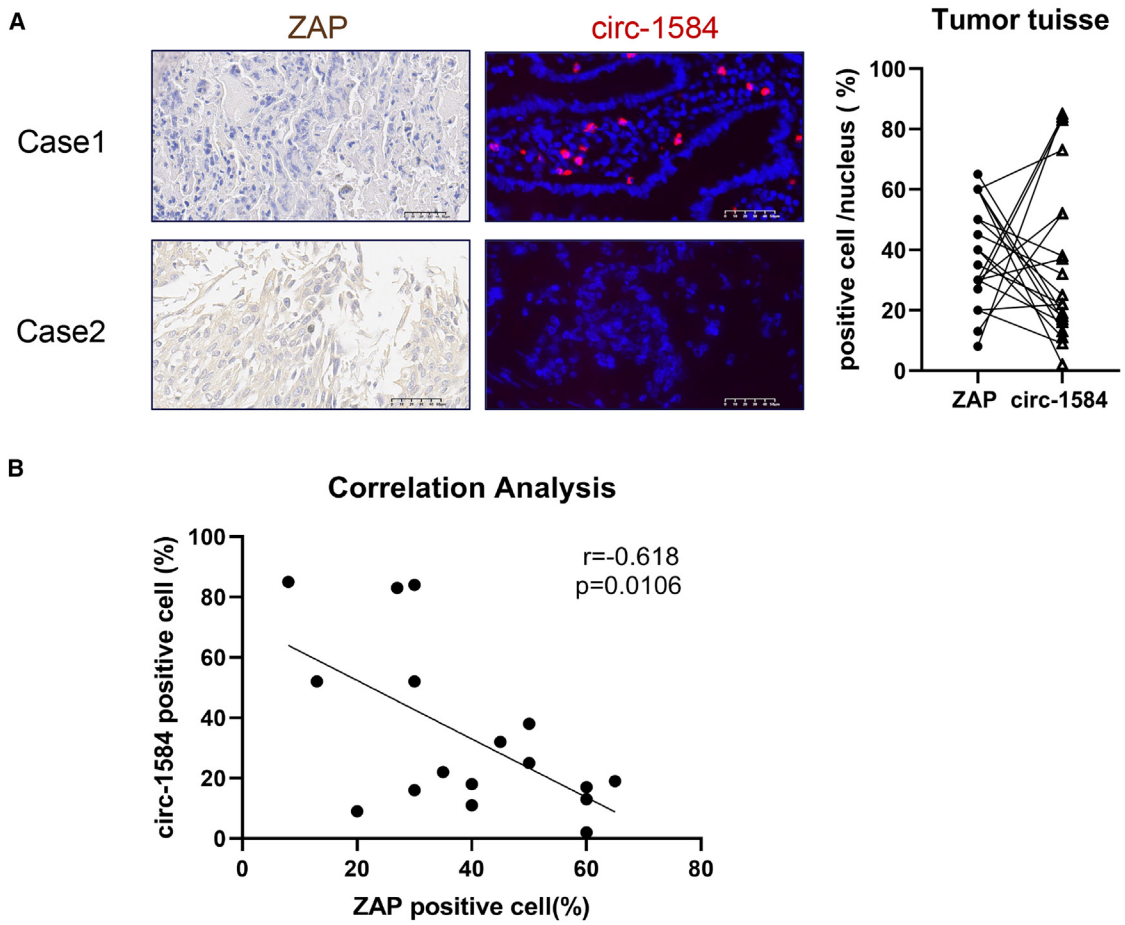

Figure 8. Negative correlation between circ-1584 and ZAP was detected in pancreatic cancer patient samples

(A) In 20 cancer tissues of pancreatic cancer patients, IHC was used to detect the expression of ZAP. FISH was used to detect the expression of circ-1584. The scale bar for the 400× photo represents 50 μm. A relative quantitative chart is shown on the right. n = 20. (B) Correlation analysis between ZAP and circ-1584; n = 17.

3,000 × g for 20 min and then filtered through a 0.45 μm filter to obtain the lentivirus. Finally, the lentivirus was concentrated in a 100 KDa ultrafiltration tube and centrifuged at 3,000 × g for 20 min to a titer of 1 × 10^8 plaque-forming units (PFUs).

The unconcentrated LV and LV-circ1584 lentivirus were infected with BxPC-3 cells, and puromycin (5 μg/mL) was screened for 10–12 days to obtain polyclonal stable strains.

Tumor model and treatment protocols

Female BALB/c nude mice aged 6–8 weeks were injected subcutaneously with 2 × 10^6 CFPAC-1 cells on the right side. On day 7, the tumors grew to an average size of 50 mm^3. Then, the tumor-bearing mice were randomized into 4 groups with 6 animals per group. The treatment strategy is shown in Figure 6A. M1 virus tail vein injection 1 × 10^7 PFU/mice, lentivirus intratumoral injection 1 × 10^7 PFU/mice. The control group received 1 × 10^7 PFU/100 μL empty lentivirus (control [CTL]), and the circ-1584 group received 1 × 10^7 PFU/100 μL circ-1584 lentivirus. The M1-treated mouse group was treated with M1 virus (1 × 10^7 PFU/300 μL) while receiving lentiviral treatment.

The tumor volume and body weight of each mouse were monitored every 3 days. Tumor volume was measured with a Vernier caliper by using the following formula: V = (length × $width^2$)/2. When tumor size reached 1,500 mm^3, mice were sacrificed. The tumor tissues and spleens of mice were collected for subsequent experiments.

The mouse experiments were performed under the protocol approved by the Animal Ethics and Welfare Committee of Sun Yat-sen University. The experiments were conducted according to the Guide for the Care and Use of Laboratory Animals, 8th Edition.

Western blotting

Tumor cells were lysed by protein lysate buffer containing protease inhibitor cocktail (TargetMol, China), proteins were extracted, and the protein concentration was detected by Bicinchoninic Acid Assay

Kit (Invitrogen, USA). Protein samples were separated by SDS-PAGE and transferred to polyvinylidene fluoride (PVDF) membranes (Millipore, USA) for immunoblotting. The PVDF membranes were incubated overnight at 4°C with primary antibodies, including GAPDH (1:1,000) (60004-1-Ig, Proteintech, China), β-actin (1:3,000, AF7018, Affinity Biosciences, China), and anti-E1 (1:1,000, produced by Beijing Protein Innovation). Then, the membranes were incubated with the corresponding horseradish peroxidase-conjugated secondary antibodies and detected with ECL Plus (Millipore, USA). Images were visualized using the ChemiDoc XRS+ System (Bio-Rad) and analyzed by the Bio-Rad Image Lab 5.2.1 software.

IHC assay

Paraffin sections of human pancreatic cancer tissue samples from the Department of Pathology of the First Affiliated Hospital of Sun Yat-sen University were deparaffinized and hydrated by xylene and ethanol gradient. Antigen retrieval was performed, and endogenous antigens were blocked by 3% hydrogen peroxide. After blocking the non-specific antigen with 3% BSA blocking solution, the sections were incubated with the ZAP antibody (1:3,000, PA5-31650, Thermo Fisher Scientific, USA) at 4°C overnight. After washing off the ZAP antibody, the sections were incubated with the secondary antibody for 20 min, followed by Diaminobenzidine staining and nuclear counterstaining. Finally, the sections were dehydrated and mounted, and image data were collected using the JiangFeng digital slide scanner.

FISH

We detected the expression of circ-1584 in paraffin-embedded sections of pancreatic cancer tissue from patients using FISH, as well as the cellular localization of circ-1584 and miR-578 in the BxPC-3 circ1584 stable cell line. The FISH experiment was performed according to the manufacturer's protocol for the FISH kit (Bes1001, Bersinbio, China). The 5′-biotin-circ-1584-3′-cy3 probe and the 5′-biotin-miR-578-3′-Fluorescein phosphoramidite (FAM)probe used for hybridization were purchased from GENCEFE. The probe sequences are listed in Table S5. The prepared fluorescent slides were photographed using a confocal electron-scanning microscope.

RNA Antisense Purification (RAP)

The biotin-conjugated circ-1584/mi-578 probes and corresponding CTL probes were used for RAP experiments. A total of 8×10^7 cells each of the circ-1584 overexpressing BxPC-3 stable cell line and the LV-BxPC-3 stable cell line were collected, and the RAP assay was performed according to the manufacturer's protocol of the RAP kit (5103-3, Bersinbio). RAP RNA was isolated with TRIzol reagent and analyzed by qPCR.

Data analysis

The data were analyzed with GraphPad Prism 8 software (GraphPad, San Diego, CA, USA). All results were expressed as the mean ± SD. The statistical significance of the differences was evaluated by a two-tailed Student's t test or a two-way ANOVA as indicated in the corresponding figure legends.

DATA AND CODE AVAILABILITY

All data generated or analyzed during this study are included in the published article.

ACKNOWLEDGMENTS

We thank all of the participants in this study. This research was funded by National Key R&D Program of China (2021YFA0909800); National Natural Science Foundation of China (82173838, 82172730, 82173837, 82203599); Guangdong Basic and Applied Basic Research Foundation (2022B1515020056, 2024A1515010317); Science and Technology Project of Guangzhou, China (No. 2023A04J0520); Medical Scientific Research Foundation of Guangdong Province, China (A2023016); Pioneering talents project of Guangzhou Development Zone, Guangdong Province (2020-L036), Guangzhou Science and Technology Plan Project (No. 2024A04J4240).

AUTHOR CONTRIBUTIONS

T.H., S.S., and J.C. wrote the manuscript. T.H., W.Z., and J.C. designed the research. T.H., Y. Li, Q.R., Y.Z., and L.G. performed the research. T.H. and J.C. analyzed the data. J.L., G.Y., Y. Lin, and J.H. supervised and edited the manuscript.

DECLARATION OF INTERESTS

The authors declare no competing interests.

SUPPLEMENTAL INFORMATION

Supplemental information can be found online at https://doi.org/10.1016/j.omton.2024.200919.

REFERENCES

1. Siegel, R.L., Giaquinto, A.N., and Jemal, A. (2024). Cancer statistics, 2024. CA Cancer J. Clin. *74*, 12–49. https://doi.org/10.3322/caac.21820.
2. Zheng, R.S., Chen, R., Han, B.F., Wang, S.M., Li, L., Sun, K.X., Zeng, H.M., Wei, W.W., and He, J. (2024). [Cancer incidence and mortality in China, 2022]. Zhonghua Zhongliu Zazhi *46*, 221–231. https://doi.org/10.3760/cma.j.cn112152-20240119-00035.
3. Zhao, C., Gao, F., Li, Q., Liu, Q., and Lin, X. (2019). The Distributional Characteristic and Growing Trend of Pancreatic Cancer in China. Pancreas *48*, 309–314. https://doi.org/10.1097/MPA.0000000000001222.
4. Chen, X., Zeh, H.J., Kang, R., Kroemer, G., and Tang, D. (2021). Cell death in pancreatic cancer: from pathogenesis to therapy. Nat. Rev. Gastroenterol. Hepatol. *18*, 804–823. https://doi.org/10.1038/s41575-021-00486-6.
5. Grossberg, A.J., Chu, L.C., Deig, C.R., Fishman, E.K., Hwang, W.L., Maitra, A., Marks, D.L., Mehta, A., Nabavizadeh, N., Simeone, D.M., et al. (2020). Multidisciplinary standards of care and recent progress in pancreatic ductal adenocarcinoma. CA Cancer J. Clin. *70*, 375–403. https://doi.org/10.3322/caac.21626.
6. Bear, A.S., Vonderheide, R.H., and O'Hara, M.H. (2020). Challenges and Opportunities for Pancreatic Cancer Immunotherapy. Cancer Cell *38*, 788–802. https://doi.org/10.1016/j.ccell.2020.08.004.
7. Chen, Y., Chen, X., Bao, W., Liu, G., Wei, W., and Ping, Y. (2024). An oncolytic virus-T cell chimera for cancer immunotherapy. Nat. Biotechnol. *42*, 1876–1887. https://doi.org/10.1038/s41587-023-02118-7.
8. Tassone, E., Muscolini, M., van Montfoort, N., and Hiscott, J. (2020). Oncolytic virotherapy for pancreatic ductal adenocarcinoma: A glimmer of hope after years of disappointment? Cytokine Growth Factor Rev. *56*, 141–148. https://doi.org/10.1016/j.cytogfr.2020.07.015.
9. Rehman, H., Silk, A.W., Kane, M.P., and Kaufman, H.L. (2016). Into the clinic: Talimogene laherparepvec (T-VEC), a first-in-class intratumoral oncolytic viral therapy. J. Immunother. Cancer *4*, 53. https://doi.org/10.1186/s40425-016-0158-5.
10. Frampton, J.E. (2022). Teserpaturev/G47Delta: First Approval. BioDrugs *36*, 667–672. https://doi.org/10.1007/s40259-022-00553-7.
11. Lin, D., Shen, Y., and Liang, T. (2023). Oncolytic virotherapy: basic principles, recent advances and future directions. Signal Transduct. Target. Ther. *8*, 156. https://doi.org/10.1038/s41392-023-01407-6.
12. Haller, S.D., Monaco, M.L., and Essani, K. (2020). The Present Status of Immuno-Oncolytic Viruses in the Treatment of Pancreatic Cancer. Viruses *12*, 1318. https://doi.org/10.3390/v12111318.

13. Sun, S., Liu, Y., He, C., Hu, W., Liu, W., Huang, X., Wu, J., Xie, F., Chen, C., Wang, J., et al. (2021). Combining NanoKnife with M1 oncolytic virus enhances anticancer activity in pancreatic cancer. Cancer Lett. *502*, 9–24. https://doi.org/10.1016/j.canlet.2020.12.018.

14. Lin, Y., Zhang, H., Liang, J., Li, K., Zhu, W., Fu, L., Wang, F., Zheng, X., Shi, H., Wu, S., et al. (2014). Identification and characterization of alphavirus M1 as a selective oncolytic virus targeting ZAP-defective human cancers. Proc. Natl. Acad. Sci. USA *111*, E4504–E4512. https://doi.org/10.1073/pnas.1408759111.

15. Guo, L., Hu, C., Liu, Y., Chen, X., Song, D., Shen, R., Liu, Z., Jia, X., Zhang, Q., Gao, Y., et al. (2023). Directed natural evolution generates a next-generation oncolytic virus with a high potency and safety profile. Nat. Commun. *14*, 3410. https://doi.org/10.1038/s41467-023-39156-3.

16. Limb, C., Liu, D.S.K., Veno, M.T., Rees, E., Krell, J., Bagwan, I.N., Giovannetti, E., Pandha, H., Strobel, O., Rockall, T.A., and Frampton, A.E. (2020). The Role of Circular RNAs in Pancreatic Ductal Adenocarcinoma and Biliary-Tract Cancers. Cancers *12*, 3250. https://doi.org/10.3390/cancers12113250.

17. Kristensen, L.S., Andersen, M.S., Stagsted, L.V.W., Ebbesen, K.K., Hansen, T.B., and Kjems, J. (2019). The biogenesis, biology and characterization of circular RNAs. Nat. Rev. Genet. *20*, 675–691. https://doi.org/10.1038/s41576-019-0158-7.

18. Wong, C.H., Lou, U.K., Fung, F.K.C., Tong, J.H.M., Zhang, C.H., To, K.F., Chan, S.L., and Chen, Y. (2022). CircRTN4 promotes pancreatic cancer progression through a novel CircRNA-miRNA-lncRNA pathway and stabilizing epithelial-mesenchymal transition protein. Mol. Cancer *21*, 10. https://doi.org/10.1186/s12943-021-01481-w.

19. Guan, H., Luo, W., Liu, Y., and Li, M. (2021). Novel circular RNA circSLIT2 facilitates the aerobic glycolysis of pancreatic ductal adenocarcinoma via miR-510-5p/c-Myc/LDHA axis. Cell Death Dis. *12*, 645. https://doi.org/10.1038/s41419-021-03918-y.

20. Wong, C.H., Lou, U.K., Li, Y., Chan, S.L., Tong, J.H., To, K.F., and Chen, Y. (2020). CircFOXK2 Promotes Growth and Metastasis of Pancreatic Ductal Adenocarcinoma by Complexing with RNA-Binding Proteins and Sponging MiR-942. Cancer Res. *80*, 2138–2149. https://doi.org/10.1158/0008-5472.CAN-19-3268.

21. Kong, Y., Li, Y., Luo, Y., Zhu, J., Zheng, H., Gao, B., Guo, X., Li, Z., Chen, R., and Chen, C. (2020). circNFIB1 inhibits lymphangiogenesis and lymphatic metastasis via the miR-486-5p/PIK3R1/VEGF-C axis in pancreatic cancer. Mol. Cancer *19*, 82. https://doi.org/10.1186/s12943-020-01205-6.

22. Zhang, X., Tan, P., Zhuang, Y., and Du, L. (2020). hsa_circRNA_001587 upregulates SLC4A4 expression to inhibit migration, invasion, and angiogenesis of pancreatic cancer cells via binding to microRNA-223. Am. J. Physiol. Gastrointest. Liver Physiol. *319*, G703–G717. https://doi.org/10.1152/ajpgi.00118.2020.

23. Xie, H., Zhao, Q., Yu, L., Lu, J., Peng, K., Xie, N., Ni, J., and Li, B. (2022). Circular RNA circ_0047744 suppresses the metastasis of pancreatic ductal adenocarcinoma by regulating the miR-21/SOCS5 axis. Biochem. Biophys. Res. Commun. *605*, 154–161. https://doi.org/10.1016/j.bbrc.2022.03.082.

24. Rong, Z., Xu, J., Shi, S., Tan, Z., Meng, Q., Hua, J., Liu, J., Zhang, B., Wang, W., Yu, X., and Liang, C. (2021). Circular RNA in pancreatic cancer: a novel avenue for the roles of diagnosis and treatment. Theranostics *11*, 2755–2769. https://doi.org/10.7150/thno.56174.

25. Maarouf, M., Wang, L., Wang, Y., Rai, K.R., Chen, Y., Fang, M., and Chen, J.L. (2023). Functional Involvement of circRNAs in the Innate Immune Responses to Viral Infection. Viruses *15*, 1697. https://doi.org/10.3390/v15081697.

26. Liu, C.X., Li, X., Nan, F., Jiang, S., Gao, X., Guo, S.K., Xue, W., Cui, Y., Dong, K., Ding, H., et al. (2019). Structure and Degradation of Circular RNAs Regulate PKR Activation in Innate Immunity. Cell *177*, 865–880.e21. https://doi.org/10.1016/j.cell.2019.03.046.

27. Qu, Z., Meng, F., Shi, J., Deng, G., Zeng, X., Ge, J., Li, Y., Liu, L., Chen, P., Jiang, Y., et al. (2021). A Novel Intronic Circular RNA Antagonizes Influenza Virus by Absorbing a microRNA That Degrades CREBBP and Accelerating IFN-beta Production. mBio *12*, e0101721. https://doi.org/10.1128/mBio.01017-21.

28. Li, X., Liu, C.X., Xue, W., Zhang, Y., Jiang, S., Yin, Q.F., Wei, J., Yao, R.W., Yang, L., and Chen, L.L. (2017). Coordinated circRNA Biogenesis and Function with NF90/NF110 in Viral Infection. Mol. Cell *67*, 214–227.e7. https://doi.org/10.1016/j.molcel.2017.05.023.

29. Shi, N., Zhang, S., Guo, Y., Yu, X., Zhao, W., Zhang, M., Guan, Z., and Duan, M. (2021). CircRNA_0050463 promotes influenza A virus replication by sponging miR-33b-5p to regulate EEF1A1. Vet. Microbiol. *254*, 108995. https://doi.org/10.1016/j.vetmic.2021.108995.

30. Chen, T.C., Tallo-Parra, M., Cao, Q.M., Kadener, S., Böttcher, R., Pérez-Vilaró, G., Boonchuen, P., Somboonwiwat, K., Díez, J., and Sarnow, P. (2020). Host-derived circular RNAs display proviral activities in Hepatitis C virus-infected cells. PLoS Pathog. *16*, e1008346. https://doi.org/10.1371/journal.ppat.1008346.

31. Zhou, W.Y., Cai, Z.R., Liu, J., Wang, D.S., Ju, H.Q., and Xu, R.H. (2020). Circular RNA: metabolism, functions and interactions with proteins. Mol. Cancer *19*, 172. https://doi.org/10.1186/s12943-020-01286-3.

32. Liu, C.X., and Chen, L.L. (2022). Circular RNAs: Characterization, cellular roles, and applications. Cell *185*, 2016–2034. https://doi.org/10.1016/j.cell.2022.04.021.

33. Nisar, M., Paracha, R.Z., Adil, S., Qureshi, S.N., and Janjua, H.A. (2022). An Extensive Review on Preclinical and Clinical Trials of Oncolytic Viruses Therapy for Pancreatic Cancer. Front. Oncol. *12*, 875188. https://doi.org/10.3389/fonc.2022.875188.

34. Pylayeva-Gupta, Y., Lee, K.E., Hajdu, C.H., Miller, G., and Bar-Sagi, D. (2012). Oncogenic Kras-induced GM-CSF production promotes the development of pancreatic neoplasia. Cancer Cell *21*, 836–847. https://doi.org/10.1016/j.ccr.2012.04.024.

35. Wang, R., Chen, J., Wang, W., Zhao, Z., Wang, H., Liu, S., Li, F., Wan, Y., Yin, J., Wang, R., et al. (2022). CD40L-armed oncolytic herpes simplex virus suppresses pancreatic ductal adenocarcinoma by facilitating the tumor microenvironment favorable to cytotoxic T cell response in the syngeneic mouse model. J. Immunother. Cancer *10*, e003809. https://doi.org/10.1136/jitc-2021-003809.

36. Yamada, T., Tateishi, R., Iwai, M., Tanaka, M., Ijichi, H., Sano, M., Koike, K., and Todo, T. (2023). Overcoming resistance of stroma-rich pancreatic cancer with focal adhesion kinase inhibitor combined with G47Delta and immune checkpoint inhibitors. Mol. Ther. Oncolytics *28*, 31–43. https://doi.org/10.1016/j.omto.2022.12.001.

37. Liu, Y., Xu, C., Xiao, X., Chen, Y., Wang, X., Liu, W., Tan, Y., Zhu, W., Hu, J., Liang, J., et al. (2022). Overcoming resistance to oncolytic virus M1 by targeting PI3K-gamma in tumor-associated myeloid cells. Mol. Ther. *30*, 3677–3693. https://doi.org/10.1016/j.ymthe.2022.05.008.

38. Danza, K., De Summa, S., Pinto, R., Pilato, B., Palumbo, O., Merla, G., Simone, G., and Tommasi, S. (2015). MiR-578 and miR-573 as potential players in BRCA-related breast cancer angiogenesis. Oncotarget *6*, 471–483. https://doi.org/10.18632/oncotarget.2509.

39. Ju, L., Luo, Y., Cui, X., Zhang, H., Chen, L., and Yao, M. (2024). CircGPC3 promotes hepatocellular carcinoma progression and metastasis by sponging miR-578 and regulating RAB7A/PSME3 expression. Sci. Rep. *14*, 7632. https://doi.org/10.1038/s41598-024-58004-y.

40. Ji, X., Shan, L., Shen, P., and He, M. (2020). Circular RNA circ_001621 promotes osteosarcoma cells proliferation and migration by sponging miR-578 and regulating VEGF expression. Cell Death Dis. *11*, 18. https://doi.org/10.1038/s41419-019-2204-y.

41. Polovitskaya, M.M., Barbini, C., Martinelli, D., Harms, F.L., Cole, F.S., Calligari, P., Bocchinfuso, G., Stella, L., Ciolfi, A., Niceta, M., et al. (2020). A Recurrent Gain-of-Function Mutation in CLCN6, Encoding the ClC-6 Cl(-)/H(+)-Exchanger, Causes Early-Onset Neurodegeneration. Am. J. Hum. Genet. *107*, 1062–1077. https://doi.org/10.1016/j.ajhg.2020.11.004.

42. He, H., Cao, X., He, F., Zhang, W., Wang, X., Peng, P., Xie, C., Yin, F., Li, D., Li, J., et al. (2024). Mutations in CLCN6 as a Novel Genetic Cause of Neuronal Ceroid Lipofuscinosis in a Murine Model. Ann. Neurol. *96*, 608–624. https://doi.org/10.1002/ana.27002.

43. Szczepaniak, J., Jagiello, J., Wierzbicki, M., Nowak, D., Sobczyk-Guzenda, A., Sosnowska, M., Jaworski, S., Daniluk, K., Szmidt, M., Witkowska-Pilaszewicz, O., et al. (2021). Reduced Graphene Oxides Modulate the Expression of Cell Receptors and Voltage-Dependent Ion Channel Genes of Glioblastoma Multiforme. Int. J. Mol. Sci. *22*, 515. https://doi.org/10.3390/ijms22020515.

44. Luo, Y., Liu, X., Li, X., Zhong, W., Lin, J., and Chen, Q. (2022). Identification and validation of a signature involving voltage-gated chloride ion channel genes for prediction of prostate cancer recurrence. Front. Endocrinol. *13*, 1001634. https://doi.org/10.3389/fendo.2022.1001634.

45. Liu, J., Wang, X., Chen, A.T., Gao, X., Himes, B.T., Zhang, H., Chen, Z., Wang, J., Sheu, W.C., Deng, G., et al. (2022). ZNF117 regulates glioblastoma stem cell differentiation towards oligodendroglial lineage. Nat. Commun. *13*, 2196. https://doi.org/10.1038/s41467-022-29884-3.

46. Colleti, C., Melo-Hanchuk, T.D., da Silva, F.R.M., Saito, Â., and Kobarg, J. (2019). Complex interactomes and post-translational modifications of the regulatory proteins HABP4 and SERBP1 suggest pleiotropic cellular functions. World J. Biol. Chem. *10*, 44–64. https://doi.org/10.4331/wjbc.v10.i3.44.

47. Goncalves, K.A., Bressan, G.C., Saito, A., Morello, L.G., Zanchin, N.I., and Kobarg, J. (2011). Evidence for the association of the human regulatory protein Ki-1/57 with the translational machinery. FEBS Lett. *585*, 2556–2560. https://doi.org/10.1016/j.febslet.2011.07.010.

48. Melo-Hanchuk, T.D., Colleti, C., Saito, Â., Mendes, M.C.S., Carvalheira, J.B.C., Vassallo, J., and Kobarg, J. (2020). Intracellular hyaluronic acid-binding protein 4 (HABP4): a candidate tumor suppressor in colorectal cancer. Oncotarget *11*, 4325–4337. https://doi.org/10.18632/oncotarget.27804.

49. Matellan, C., Lachowski, D., Cortes, E., Chiam, K.N., Krstic, A., Thorpe, S.D., and Del Río Hernández, A.E. (2023). Retinoic acid receptor beta modulates mechanosensing and invasion in pancreatic cancer cells via myosin light chain 2. Oncogenesis *12*, 23. https://doi.org/10.1038/s41389-023-00467-1.